



SAKARYA ÜNİVERSİTESİ

FEN BİLİMLERİ ENSTİTÜSÜ DERGİSİ

Sakarya University Journal of Science
SAUJS

ISSN 1301-4048 e-ISSN 2147-835X Period Bimonthly Founded 1997 Publisher Sakarya University
<http://www.saujs.sakarya.edu.tr/>

Title: Facile Synthesis And Characterization Of gCN, gCN-Zn And gCN-Fe Binary Nanocomposite And Its Application As Photocatalyst For Methylene Blue Degradation

Authors: Mustafa KAVGACI, Hasan ESKALEN

Received: 2022-10-28 00:00:00

Accepted: 2023-02-23 00:00:00

Article Type: Research Article

Volume: 27

Issue: 3

Month: June

Year: 2023

Pages: 530-541

How to cite

Mustafa KAVGACI, Hasan ESKALEN; (2023), Facile Synthesis And Characterization Of gCN, gCN-Zn And gCN-Fe Binary Nanocomposite And Its Application As Photocatalyst For Methylene Blue Degradation. Sakarya University Journal of Science, 27(3), 530-541, DOI: 10.16984/saufenbilder.1195934

Access link

<https://dergipark.org.tr/en/pub/saufenbilder/issue/78131/1195934>

New submission to SAUJS

<http://dergipark.gov.tr/journal/1115/submission/start>

Facile Synthesis and Characterization of gCN, gCN-Zn and gCN-Fe Binary Nanocomposite and Its Application as Photocatalyst for Methylene Blue Degradation

Mustafa KAVGACI^{*1,3} , Hasan ESKALEN^{2,3} 

Abstract

The combustion method to obtain for pure graphitic carbon nitride (gCN) and two binary nanocomposites, gCN-Zn - gCN-Fe have been used in the present study. The structural, morphological, thermal and optical characterizations of the synthesized samples were characterized with X-ray diffraction, scanning electron microscopy, thermogravimetric analysis (TGA) and UV-Vis spectroscopy. The intensity of characteristic gCN peak at (002) crystalline plane decrease with formation of binary nanocomposites was observed. The EDX spectra supports presents of Zn and Fe element in binary nanocomposites. The bandgap of pristine gCN is calculated as 2.75 eV and it decreases to 2.58 eV and 2.50 eV for Zn and Fe addition. The degradation capacity of pristine gCN and synthesized binary nanocomposites showed an enhanced photodegradation performance for binary composite relative to pristine gCN was observed. The maximum degradation performance was observed at gCN-Zn binary composite. The obtained composites with this simple synthesis method and cost effective raw materials used for the photodegradation of methylene blue dye detail.

Keywords: Degradation, Zn, Fe, methylene blue (MB), graphitic carbon nitride (gCN)

1. INTRODUCTION

Environmental pollution is one of the significant problems for humans and other living organisms. Unfortunately, pollution increases in parallel to industrialization, which might result in pollution of water sources and unhealthy drinking water. To overcome this problem, some scientists focused on water treatment, especially

pollution originating from dyestuff. Since the wastewater from dye can contaminate not only freshwater sources but also sands, that may magnify the risk [1–5]. Some of the organics dyes are toxic, carcinogenic, and have mutagenic potential [6]. Considering the current situation of dyes, especially their types (more than 100,000 varied structured) and different application areas (textile, medicine, pharmaceutical, cosmetics, food,

* Corresponding author: mkavgaci@gmail.com (M. KAVGACI)

¹ Elbistan Vocational School of Health Services, Department of Opticianry, Kahramanmaraş Istiklal University, Kahramanmaraş, Turkey.

² Vocational School of Health Services, Department of Opticianry, Kahramanmaraş Sutcu Imam University, Kahramanmaraş, Turkey.

³ Department of Material Science and Engineering, Graduate School of Natural and Applied Sciences, Kahramanmaraş Sutcu Imam University, Kahramanmaraş, Turkey.

E-Mail: heskalen@gmail.com

ORCID: <https://orcid.org/0000-0001-8747-0635>, <https://orcid.org/0000-0002-4523-6573>



printing), the importance of treatment of wastewater originating from dyes may become more evident [7–9]. Different methods have been utilized to degrade wastewater, including physiochemical and biological approaches; photodegradation has massive potential for dealing with wastewater since its a clean and cost-effective method [10–12].

Graphitic carbon nitride (gCN) is defined as nitrogen substituted graphane with anisotropic 2D geometry, and aromatic conjugate structure [13]. gCN has been considered as a promotion material due to its original preparation methods, high stability, band gap and low cost [14–16]. Moreover, the earth abundant nature, suitable electronic band position, nontoxic characteristic, outstanding physicochemical stability and admirable optical properties has considered as novel specifications of the gCN [17, 18]. Triurea, melamine, cyanamide, urea, ammonium thiocyanate and dicyandiamide are some examples of gCN precursors that are inexpensive and high nitrogen content generally used in synthesis of gCN [17]. Fast charge carrier recombination, small particle size and poor absorption coefficient of the gCN negatively affect the photoactivity of pure gCN [19–21]. Different methods have been utilized to overcome this shortcoming like fabricating nano/mesoporous structures, coupling with other semiconductors, noble metal deposition and impurity doping [22–24]. Among them doping different elements like metal, metal oxide and nonmetals to the bulk structure results in a decrease in band gap and lead to enhancement of absorption of visible light [25]. Flower like copper/zinc bedecked gCN composite (gCN-CuO/ZnO) was fabricated and methylene blue dye (MB) degradation was investigated. The enhancement of the photocatalytic activity of gCN-CuO/ZnO relative to pure gCN has been observed [26]. H₂ release of P doped gCN - TiO₂ catalyst was used for hydrogen (H₂) release from the sodium borohydride (NaBH₄) methanolysis [27]. The photocatalytic degradation of Rhodamine B

dye of gCN/nano zero valent iron doped bismuth ferrite nanoparticle composite demonstrated the degradation performance better than previously reported BiFeO₃ composite [28]. The photocatalytic performance of silver iodide- gCN nanocomposite was exhibited better behavior than pristine silver iodide and gCN over rhodamine B and methyl orange dye was reported [29]. Enhanced photocatalytic behavior observed with the addition of reduced graphene oxide and gCN to zinc oxide over methylene blue dye was investigated [30].

The present work has employed the combustion method to obtain two binary nanocomposites, gCN-Zn and gCN-Fe. The structural, morphological, thermal and optical characterizations were performed in detail. The degradation capacity of pristine gCN and synthesized binary nanocomposites showed an enhanced photodegradation performance for binary composite relative to pristine gCN was observed. The obtained composites with this simple synthesis method and cost effective raw materials used for the photodegradation of methylene blue dye detail.

2. MATERIALS AND METHOD

2. 1. Materials

Ultra pure water was used in the studies. Ultra pure water was obtained from Kahramanmaraş Sutcu Imam University University-Industry-Public Cooperation Development Application and Research Center (USKIM). All chemicals were used in tests and syntheses without purification. Thiourea (98%) was purchased from Merck, zinc nitrate (98%) was from Acros Organics, and iron nitrate (99%) was from Sigma Aldrich.

2. 2. Synthesis of gCN, gCN-Fe and gCN-Zn

gCN was produced using a the combustion method. Thiourea (10 g) in a ceramic crucible was heated to 550 °C at a heating rate of 10 °C/min in an muffle furnace. It was then calcined at 550 °C for 5 hours. gCN-Fe and gCN-Zn were synthesized under the same conditions. Briefly, 10 g of thiorue was dissolved in 50 mL of ultra water. Iron nitrate and zinc nitrate were then added to this solution in a weight ratio of 0.25:10. It was mixed on a magnetic stirrer for 1 hour. It was then dried at 90 °C for 48 hours. The obtained powder sample was heated to 550 °C at a heating rate of 5 °C/min and calcined at the same temperature for 5 hours. The synthesized samples were ground in a mortar for experiments. The graphitic carbon nitride gCN synthesized in a weight ratio of 0.25:10 was named as iron-doped graphitic carbon nitride gCN-Fe and zinc-doped graphitic carbon nitride gCN-Zn. Figure 1 shows a graphical representation of the gCN samples synthesis.

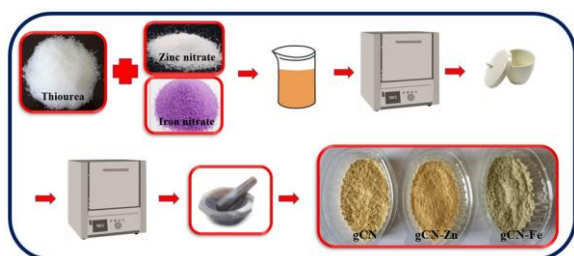


Figure 1 Scheme showing synthesis of gCN, gCN-Fe and gCN-Zn samples

2.3.Characterization

The X-ray diffraction (XRD) pattern of the gCN samples was obtained using a Philips brand X'Pert PRO model XRD instrument with Cu Ka radiation ($\lambda=0.154056$ nm, 40 kV and 30 mA). Scanning Electron Microscope (SEM) images and EDX measurements were taken with the FEI brand Quanta 650 Field Emission SEM model electron microscope available at Çukurova University Central Research Laboratory (CUMERLAB). Thermogravimetric analysis (TGA) was

performed using a thermal analyzer (Perkin-Elmer Diamond) in a nitrogen atmosphere with a heating rate of 20 °C/min in the temperature range of 20 to 750 °C. FT-IR spectrum measurements were taken with the Perkin Elmer Spectrum 400 device in the range of 4000–400 cm^{-1} . UV–Vis absorption measurements were obtained with a Shimadzu-1800 UV spectrometer. XRD, TGA, FTIR and UV measurements were obtained in the USKIM laboratory.

2.4. Photocatalytic test

The photocatalytic performance of the produced gCN, gCN-Fe and gCN-Zn structures was tested with methylene blue (MB) dye. 20 mg of the photocatalyst gCN, 5 ppm was dropped into 50 mL MB solution (with water). First of all, the solutions to which the catalyst was added were kept in the dark for 30 minutes, taking into account the absorption-desorption balance. It was then tested by irradiation under a Xeon lamp light source (300 W Luzchem). Photocatalytic performances of the samples were investigated with a Shimadzu UV1800 spectrometer in 10-minute time [.

3. RESULTS AND DISCUSSION

Graphically showing the XRD patterns of gCN, gCN-Fe and gCN-Zn are presented (Figure 2). Two characteristic peaks of pure gCN appear prominently at 12.8° and 27.3° both (100) and (002) peaks can be attributed to interplanetary structural stacking of conjugated aromatic systems indexed for graphite materials. These peaks are consistent with the XRD data of the reported studies available in the literature for the gCN structure [31, 32]. It is clearly seen in the XRD graph that the intensity of the (002) peak decreases with the doping of Zn and Fe. This suggests that adding Zn and Fe can limit the crystal growth of gCN. The decrease in peak intensity can be attributed to an interaction between Zn/Fe and gCN. This effect deforms the nitride pore structure and changes the distance between the holes [33]. In addition,

the decrease in crystallinity in the (002) crystal planes can be attributed to the effects of Fe and Zn additions on the thermal condensation of urea/thiourea [34]. When the XRD graph was examined, no diffraction peak was observed for Zn and Fe structures.

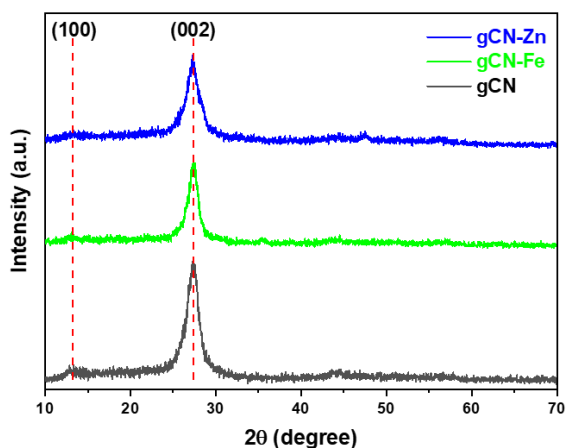


Figure 2 XRD pattern of gCN, gCN-Fe and gCN-Zn

SEM images illuminating the SEM surface morphologies of gCN, gCN-Fe and gCN-Zn are given in Figure 3. Characteristic plate-like structures are seen and the construction of pronounced 2D layered bulk sheets that remain grouped together is clearly seen from this figure. Fe and Zn additives did not affect gCN morphology [35]. This demonstrates that introducing Fe to gCN does not modify its sheet structure. According to result of similar research related to 5% Fe doped gCN that obtained composite not contain any iron nanoparticles, proving that Fe was ionically added to the gCN framework [36]. The addition of Fe to the carbon nitride structure does not alter the stacking of chain layers, implying that Fe-gCN preserves the original crystal structure of gCN [37]. The morphology of ZnO incorporated gCN was observed by SEM and the images reveal its 2-D layered nanosheet structures without much variation in its morphology upon incorporating zinc metal into gCN.

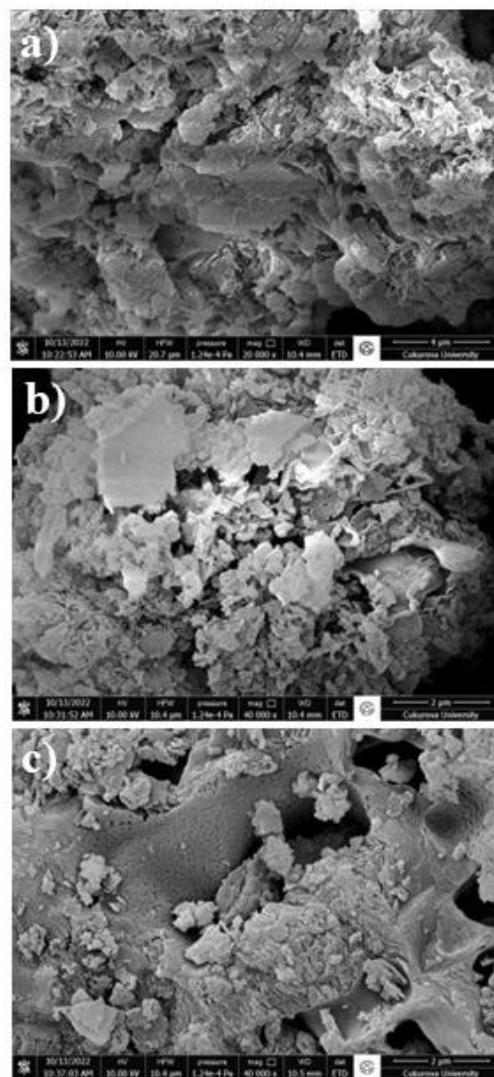


Figure 3 SEM images of gCN (a) gCN-Fe (b) and gCN-Zn (c)

EDX analysis was performed to determine the chemical composition of gCN, gCN-Fe and gCN-Zn nanocatalysts (Figure 4). The EDX spectra of the samples confirm the presence of C, N, O, Fe and Zn elements.

Optical band gap energies of the synthesized samples were determined by using optical absorption spectra. Optical band gaps were obtained with the Tauc plot. $(\alpha h\nu)^2$ for samples as a function of photon energy is plotted graphically in Figure 5. The band gap energy for gCN was found to be 2.75 eV. In the literature, some researchers found the same result for gCN [38, 39]. The addition of Zn and Fe decreased the band gap energy. Band gap energies for gCN-Zn and gCN-Fe

were found to be 2.58 eV and 2.50 eV, respectively. The results found are in agreement with previous studies. In the literature, some studies found that the forbidden energy gap decreases with the addition of Zn and Fe to gCN [33, 40, 41].

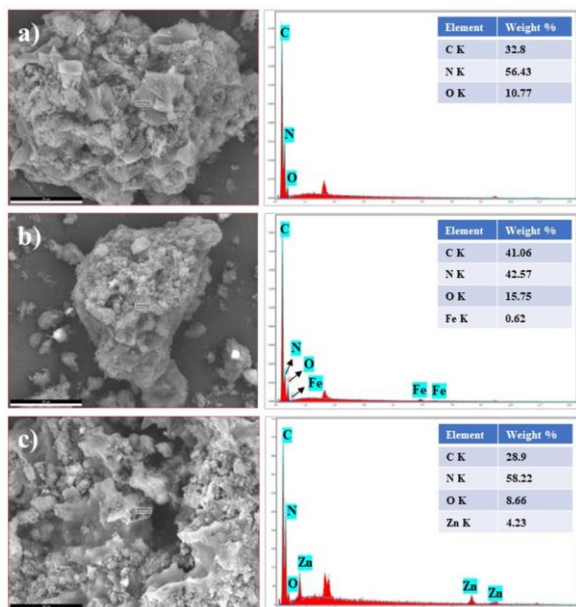


Figure 4 EDX spectra of gCN (a) gCN-Fe (b) and gCN-Zn (c)

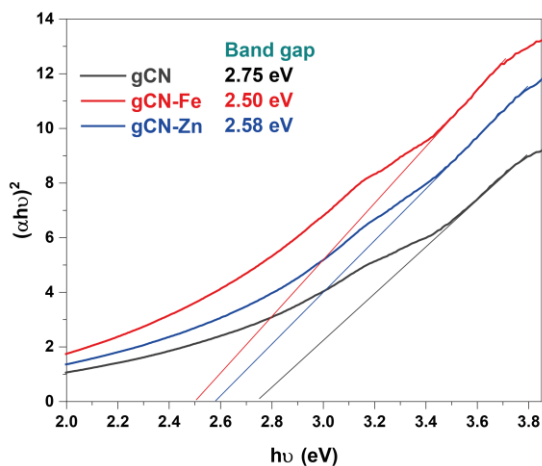


Figure 5 Bandgap graph gCN, gCN-Fe and gCN-Zn

The TGA pattern of gCN, gCN-Fe and gCN-Zn are presented in Figure 6. It is observed that the remarkable thermal decomposition of the samples starts around 400 °C. It is clearly seen that the samples show a tendency to decompose at temperatures higher than 600 °C. This result indicates that thermally gCN structures are one of the highly stable organic

materials [42]. The degree of condensation seriously affects thermal stability. Complete degradation of the synthesized gCN sample takes place at 620 °C and no material remains. However, complete degradation does not occur in Zn and Fe doped gCN samples.

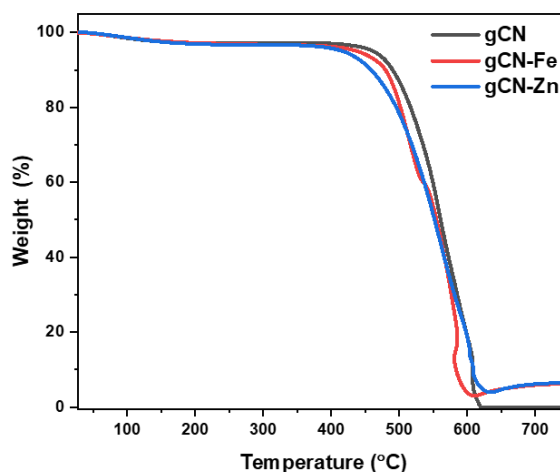


Figure 6 TG thermograms for the gCN, gCN-Fe and gCN-Zn

FTIR spectroscopy is used to detect tensile and bending vibrational bands of synthesized gCN structures and to examine the functional groups and types of chemical bonds of gCN structures. Figure 7 shows the FT-IR spectra of the synthesized gCN constructs. Measurements in the range of 450–4000 cm^{-1} were taken for the FTIR analysis. The broad absorption peak centered at 3150 cm^{-1} is attributed to the tensile vibration of the N–H group. The peaks seen in the 1000–1750 cm^{-1} range indicate the characteristic stretching modes of C–N heterocycles. The sharp peak observed at 805 cm^{-1} can be assigned to the respiratory mode typical of triazine units [43, 44]. As a result of the addition of Zn and Fe, the intensity of the peaks observed between 3150 cm^{-1} and 1000–1750 cm^{-1} decreased. This indicates that the crystallization of Fe and Zn can affect the thermal polymerization of Thiourea. It is consistent with the result of the XRD analysis, which shows that the addition of Fe and Zn can lead to the deterioration of the graphite structure of gCN [33].

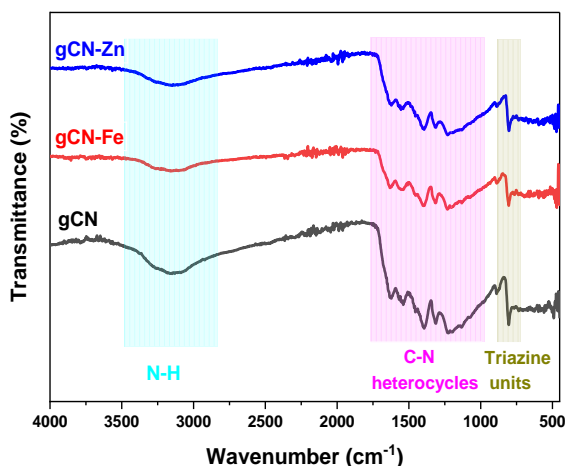


Figure 7 FTIR pattern of obtained samples

Optical absorptions of synthesized gCN samples were measured between 450-750 nm wavelengths using UV-vis spectroscopy. All samples were kept in the dark for 30 minutes and then measurements were taken with a UV-Vis spectrophotometer every 10 minutes for 60 minutes. The photocatalytic degradation of the catalyst-free and gCN-catalyzed dyestuff solutions with respect to time was investigated under normal conditions under 300 W Xenon light. In Figure 8, absorption graphs of gCN, gCN-Fe and gCN-Zn samples are given. The maximum peak in the UV-Vis absorption spectra of the dyestuffs was determined as 664 nm for methylene blue. 50 ml of 5 ppm methylene blue solution was taken and kept under xenon and room light for 60 minutes without a catalyst. The degradation rates under room conditions (called day in Figure 9) and under a xenon lamp (called sim in Figure 9) were determined as 2.7% and 5.4%, respectively (Figure 9).

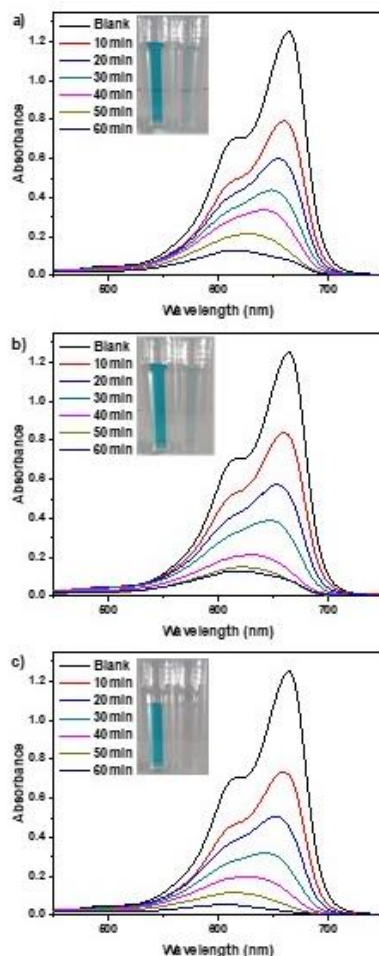


Figure 8 UV-visible absorption spectra for MB in a) gCN, b) gCN-Fe and c) gCN-Zn

In Figure 9, the graph of the decay rates with respect to time is given. In Figure 9, the degradation rates of gCN samples on MB after 60 minutes were determined as 92.7% for gCN, 93.3% for gCN-Fe and 98.4% for gCN-Zn.

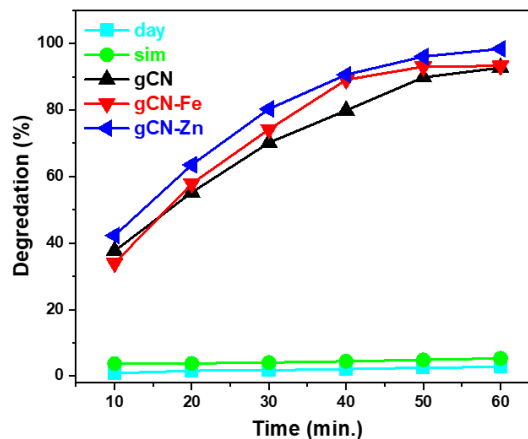


Figure 9 The degradation graph of MB in all samples

It was observed that the synthesized Zn-doped gCN sample was more effective on MB. Figure 10 presents the graph of $\ln(C_0/C_t)$ versus time. k (min^{-1}) rate constants (pseudo-first order) were calculated using the slope of the graphs [45]. As can be seen from the graph, the gCN-Zn sample with the highest degradation rate has the largest k value ($k=0,06839 \text{ min}^{-1}$).

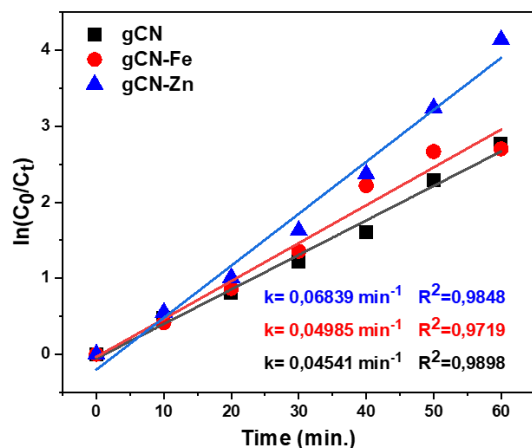


Figure 10 Graph of $\ln(C_0/C_t)$ to time gCN, gCN-Fe and gCN-Zn

Photocatalytic evaluation of prepared gCN, gCN-Fe and gCN-Zn samples was investigated through the degradation of MB. gCN-Fe and gCN-Zn were found to exhibit better photocatalytic activity compared to pure gCN. The primary factors of photocatalytic activity are light-absorption capacity, surface composition, and photogenerated charge-separation efficiency [46]. The improvement in photocatalytic activity of gCN-Fe and gCN-Zn composites can be attributed to (i) gCN-Fe and gCN-Zn have a well-developed synergistic interaction in the obtained structure, (ii) a reduction in the bandgap energy of a binary composite can increase the transfer of photo-induced electrons while decreasing electron-hole pair recombination [47, 48]. Zinc oxide absorbs more light quanta than iron oxide and this may be the reason of the synthesized gCN-Zn shows better performance than the gCN-Fe sample [49]. This can increase photocatalytic activity. In addition, the development of photocatalytic activity can be attributed to the

promotion of hydroxyl radical formation [40, 41, 50–52].

4. CONCLUSION

In summary, the pristine gCN, gCN-Zn and gCN-Fe structures were successfully synthesized by the combustion method. The structural properties of the obtained samples were detailedly characterized with X-Ray diffraction, SEM-EDX, FTIR and UV-Vis spectroscopy. The bandgap value of pure gCN was found as 2.75 eV and the band gap values of gCN-Zn and gCN-Fe synthesized binary composites decrease to 2.58 eV and 2.50 eV respectively. The results of the elemental analysis show the apparent differences between the pure forms of gCN, gCN-Zn, and gCN-Fe indicating that synthesized binary composites have different composition. The obtained FTIR results are comparable with the XRD study, which reveals that the addition of Fe and Zn can cause the graphite structure of gCN to deteriorate. The photocatalytic performances of the synthesized materials were investigated. The degradation effect of synthesized nanocomposites on MB was enhanced with metal ion doping. The obtained results also demonstrated that adding a zinc and iron elements increased the photocatalytic activity remarkably. Among the samples examined, gCN-Zn exhibited the highest photocatalytic performance. The degradation effect of gCN-Zn sample on MB was found to be 98.4% after 60 minutes. The results showed strong photocatalytic effects of Fe and Zn doped gCN structures. Therefore, the prepared gCN-Zn nanocomposite has significant potential and a promising candidate for the destruction of environmental pollutants.

Funding

This work was financially supported by Kahramanmaraş Sütçü İmam University, (KSU) Scientific Research Projects Coordination Department, under Project No. 2021/1-7 YLS and 2020/3-7 YLS.

Authors' Contribution

The authors contributed equally to the study.

The Declaration of Conflict of Interest/ Common Interest

No conflict of interest or common interest has been declared by the authors.

The Declaration of Ethics Committee Approval

This study does not require ethics committee permission or any special permission.

The Declaration of Research and Publication Ethics

The authors of the paper declare that they comply with the scientific, ethical and quotation rules of SAUJS in all processes of the paper and that they do not make any

REFERENCES

- [1] S. Kerli, H. Eskalen, "Synthesis of titanium oxide thin films by spray pyrolysis method and its photocatalytic activity for degradation of dyes and ciprofloxacin," *Physics and Chemistry of Solid State*, vol. 21, no. 3, pp. 426–432, 2020.
- [2] H. Eskalen, S. Uruş, Ş. Özgan, "Microwave-Assisted Synthesis of Mushrooms Like MWCNT/SiO₂@ZnO Nanocomposite: Influence on Nematic Liquid Crystal E7 and Highly Effective Photocatalytic Activity in Degradation of Methyl Blue," *Journal of Inorganic and Organometallic Polymers and Materials*, vol. 31, no. 2, pp. 763–775, 2021.
- [3] H. Eskalen, H. Yaykaşlı, M. Kavgacı, A. Kayış, "Investigating the PVA/TiO₂/CDs polymer nanocomposites: effect of carbon dots for photocatalytic degradation of Rhodamine B," *Journal of Materials Science: Materials in Electronics*, vol. 33, no. 7, pp. 4643–4658, 2022.
- [4] S. Uruş, M. Çaylar, H. Eskalen, Ş. Özgan, "Synthesis of GO@Fe₃O₄@TiO₂ type organic–inorganic nanohybrid material: Investigation of the effect of nanohybrid doped liquid crystal E7 and the photocatalytic degradation of ciprofloxacin," *Journal of Materials Science: Materials in Electronics*, vol. 33, no. 7, pp. 4314–4329, 2022.
- [5] H. Eskalen, S. Kerli, "Synthesis of Gd Doped TiO₂ Thin Film for Photocatalytic Degradation of Malachite Green," *Sakarya University Journal of Science*, vol. 24, no. 6, pp. 1210–1215, 2020.
- [6] M. Ikram, F. Jamal, A. Haider, S. Dilpazir, T. Shujah, M. Naz, M. Imran, A. Ul-Hamid, I. Shahzadi, H. Ullah, W. Nabgan, S. Ali, "Efficient Photocatalytic Dye Degradation and Bacterial Inactivation by Graphitic Carbon Nitride and Starch-Doped Magnesium Hydroxide Nanostructures," *ACS Omega*, p. 2022.
- [7] S. Kerli, Ü. Alver, H. Eskalen, S. Uruş, A.K. Soğuksu, "Structural and Morphological Properties of Boron Doped V₂O₅ Thin Films: Highly Efficient Photocatalytic Degradation of Methyl Blue," *Russian Journal of Applied Chemistry* 2019 92:2, vol. 92, no. 2, pp. 304–309, 2019.
- [8] C. Kursun, M. Gogebakan, H. Eskalen, S. Uruş, J.H. Perepezko, "Microstructural Evaluation and Highly Efficient Photocatalytic Degradation Characteristic of Nanostructured Mg₆₅Ni₂₀Y₁₅–xLa_x (X = 1, 2, 3) Alloys," *Journal of Inorganic and Organometallic Polymers and Materials*, vol. 30, no. 2, pp. 494–503, 2020.

- [9] H. Eskalen, S. Uruş, H. Yaykaşlı, M. Gögebakan, "Microstructural Characterization of Ball Milled Co₆₀Fe₁₈Ti₁₈Nb₄ Alloys and Their Photocatalytic Performance," *Alloy Materials and Their Allied Applications*, pp. 91–103, 2020.
- [10] N. Venkatesh, G. Murugadoss, A.A.A. Mohamed, M.R. Kumar, S.G. Peera, P. Sakthivel, "A Novel Nanocomposite Based on Triazine Based Covalent Organic Polymer Blended with Porous g-C₃N₄ for Photo Catalytic Dye Degradation of Rose Bengal and Fast Green," *Molecules* 2022, Vol. 27, Page 7168, vol. 27, no. 21, p. 7168, 2022.
- [11] H. Özlü Torun, R. Kırkgeçit, F. Kılıç Dokan, E. Öztürk, "Preparation of La-Dy-CeO₂ ternary compound: Examination of photocatalytic and photoluminescence properties," *Journal of Photochemistry and Photobiology A: Chemistry*, vol. 418, p. 113338, 2021.
- [12] M. Atashkadi, A. Mohadesi, M.A. Karimi, S.Z. Mohammadi, V. Haji Aghaei, "Synthesis and characterization of Black Au nanoparticles deposited over g-C₃N₄ nanosheets: enhanced photocatalytic degradation of methylene blue," *Environmental Technology*, pp. 1–17, 2022.
- [13] V. Ugraskan, F. Karaman, "Enhanced thermoelectric properties of highly conductive poly (3,4-ethylenedioxy thiophene)/exfoliated graphitic carbon nitride composites," *Synthetic Metals*, vol. 287, p. 117070, 2022.
- [14] S. Yılmaz, E.G. Acar, G. Yanalak, E. Aslan, M. Kılıç, İ. Hatay Patır, Ö. Metin, "Enhanced hydrogen evolution by using ternary nanocomposites of mesoporous carbon nitride/black phosphorous/transition metal nanoparticles (m-gCN/BP-M; M = Co, Ni, and Cu) as photocatalysts under visible light: A comparative experimental and theoretical study," *Applied Surface Science*, vol. 593, p. 153398, 2022.
- [15] A. Sudhaik, P. Raizada, S. Thakur, A.K. Saini, P. Singh, A. Hosseini-Bandegharai, "Metal-free photo-activation of peroxy monosulfate using graphene supported graphitic carbon nitride for enhancing photocatalytic activity," *Materials Letters*, vol. 277, p. 128277, 2020.
- [16] G. K. Dutta, N. Karak, "Bio-based waterborne polyester supported oxygenous graphitic carbon nitride nanosheets as a sustainable photocatalyst for aquatic environment remediation," *Journal of Cleaner Production*, vol. 285, p. 124906, 2021.
- [17] M. S. Khan, F. Zhang, M. Osada, S. S. Mao, S. Shen, "Graphitic Carbon Nitride-Based Low-Dimensional Heterostructures for Photocatalytic Applications," *Solar RRL*, vol. 4, no. 8, p. 1900435, 2020.
- [18] W. Xu, S. Lai, S. C. Pillai, W. Chu, Y. Hu, X. Jiang, M. Fu, X. Wu, F. Li, H. Wang, "Visible light photocatalytic degradation of tetracycline with porous Ag/graphite carbon nitride plasmonic composite: Degradation pathways and mechanism," *Journal of Colloid and Interface Science*, vol. 574, pp. 110–121, 2020.
- [19] V. Balakumar, R. Manivannan, C. Chuaicham, S. Karthikeyan, K. Sasaki, "A simple tactic synthesis of hollow porous graphitic carbon nitride with significantly enhanced photocatalytic performance," *Chemical Communications*, vol. 57, no. 55, pp. 6772–6775, 2021.

- [20] J. Tan, Z. Li, J. Li, Y. Meng, X. Yao, Y. Wang, Y. Lu, T. Zhang, "Visible-light-assisted peroxymonosulfate activation by metal-free bifunctional oxygen-doped graphitic carbon nitride for enhanced degradation of imidacloprid: Role of non-photochemical and photocatalytic activation pathway," *Journal of Hazardous Materials*, vol. 423, p. 127048, 2022.
- [21] D. Gogoi, A. K. Shah, M. Qureshi, A. K. Golder, N. R. Peela, "Silver grafted graphitic-carbon nitride ternary heterojunction Ag /gC₃N₄(Urea) -gC₃N₄ (Thiourea) with efficient charge transfer for enhanced visible-light photocatalytic green H₂ production," *Applied Surface Science*, vol. 558, p. 149900, 2021.
- [22] R. Kavitha, P. M. Nithya, S. Girish Kumar, "Noble metal deposited graphitic carbon nitride based heterojunction photocatalysts," *Applied Surface Science*, vol. 508, p. 145142, 2020.
- [23] N. Rono, J. K. Kibet, B. S. Martincigh, V. O. Nyamori, "A comparative study between thermal etching and liquid exfoliation of bulk graphitic carbon nitride to nanosheets for the photocatalytic degradation of a model environmental pollutant, Rhodamine B," *Journal of Materials Science: Materials in Electronics*, vol. 32, no. 1, pp. 687–706, 2021.
- [24] H. Lin, X. Tang, J. Wang, Q. Zeng, H. Chen, W. Ren, J. Sun, H. Zhang, "Enhanced visible-light photocatalysis of clofibric acid using graphitic carbon nitride modified by cerium oxide nanoparticles," *Journal of Hazardous Materials*, vol. 405, p. 124204, 2021.
- [25] A. Hayat, A. G. Al-Sehemi, K. S. El-Nasser, T. A. Taha, A. A. Al-Ghamdi, Jawad Ali Shah Syed, M. A. Amin, T. Ali, T. Bashir, A. Palamanit, J. Khan, W. I. Nawawi, "Graphitic carbon nitride (g-C₃N₄)-based semiconductor as a beneficial candidate in photocatalysis diversity," *International Journal of Hydrogen Energy*, vol. 47, no. 8, pp. 5142–5191, 2022.
- [26] S. Sivasakthi, K. Gurunathan, "Graphitic carbon nitride bedecked with CuO/ZnO hetero-interface microflower towards high photocatalytic performance," *Renewable Energy*, vol. 159, pp. 786–800, 2020.
- [27] C. Saka, "Phosphorus decorated g-C₃N₄-TiO₂ particles as efficient metal-free catalysts for hydrogen release by NaBH₄ methanolysis," *Fuel*, vol. 322, p. 124196, 2022.
- [28] M. U. Rahman, U. Y. Qazi, T. Hussain, N. Nadeem, M. Zahid, H. N. Bhatti, I. Shahid, "Solar driven photocatalytic degradation potential of novel graphitic carbon nitride based nano zero-valent iron doped bismuth ferrite ternary composite," *Optical Materials*, vol. 120, p. 111408, 2021.
- [29] Y. Orooji, M. Ghanbari, O. Amiri, M. Salavati-Niasari, "Facile fabrication of silver iodide/graphitic carbon nitride nanocomposites by notable photocatalytic performance through sunlight and antimicrobial activity," *Journal of Hazardous Materials*, vol. 389, p. 122079, 2020.
- [30] U. Saeed, A. Jilani, J. Iqbal, H. Al-Turaif, "Reduced graphene oxide-assisted graphitic carbon nitride@ZnO rods for enhanced physical and photocatalytic degradation," *Inorganic Chemistry Communications*, vol. 142, p. 109623, 2022.

- [31] L. Ge, "Synthesis and photocatalytic performance of novel metal-free g-C₃N₄ photocatalysts," *Materials Letters*, vol. 65, no. 17–18, pp. 2652–2654, 2011.
- [32] H. Zou, X. Yan, J. Ren, X. Wu, Y. Dai, D. Sha, J. Pan, J. Liu, "Photocatalytic activity enhancement of modified g-C₃N₄ by ionothermal copolymerization," *Journal of Materiomics*, vol. 1, no. 4, pp. 340–347, 2015.
- [33] D. R. Paul, S. Gautam, P. Panchal, S. P. Nehra, P. Choudhary, A. Sharma, "ZnO-Modified g-C₃N₄: A Potential Photocatalyst for Environmental Application," *ACS Omega*, vol. 5, no. 8, pp. 3828–3838, 2020.
- [34] J. Hu, P. Zhang, W. An, L. Liu, Y. Liang, W. Cui, "In-situ Fe-doped g-C₃N₄ heterogeneous catalyst via photocatalysis-Fenton reaction with enriched photocatalytic performance for removal of complex wastewater," *Applied Catalysis B: Environmental*, vol. 245, pp. 130–142, 2019.
- [35] M. Piri, M. M. Heravi, A. Elhampour, F. Nemati, "Silver nanoparticles supported on P, Se-codoped g-C₃N₄ nanosheet as a novel heterogeneous catalyst for reduction of nitroaromatics to their corresponding amines," *Journal of Molecular Structure*, vol. 1242, p. 130646, 2021.
- [36] J. Hu, P. Zhang, W. An, L. Liu, Y. Liang, W. Cui, "In-situ Fe-doped g-C₃N₄ heterogeneous catalyst via photocatalysis-Fenton reaction with enriched photocatalytic performance for removal of complex wastewater," *Applied Catalysis B: Environmental*, vol. 245, pp. 130–142, 2019.
- [37] Y. Oh, J.O. Hwang, E.S. Lee, M. Yoon, V.D. Le, Y.H. Kim, D.H. Kim, S.O. Kim, "Divalent Fe Atom Coordination in Two-Dimensional Microporous Graphitic Carbon Nitride," *ACS Applied Materials and Interfaces*, vol. 8, no. 38, pp. 25438–25443, 2016.
- [38] C. Liu, H. Huang, W. Cui, F. Dong, Y. Zhang, "Band structure engineering and efficient charge transport in oxygen substituted g-C₃N₄ for superior photocatalytic hydrogen evolution," *Applied Catalysis B: Environmental*, vol. 230, pp. 115–124, 2018.
- [39] M. A. Mohamed, M. F. M. Zain, L. Jeffery Minggu, M. B. Kassim, N. A. Saidina Amin, W. N. W. Salleh, M. N. I. Salehmin, M. F. Md Nasir, Z. A. Mohd Hir, "Constructing bio-templated 3D porous microtubular C-doped g-C₃N₄ with tunable band structure and enhanced charge carrier separation," *Applied Catalysis B: Environmental*, vol. 236, pp. 265–279, 2018.
- [40] S. Babar, N. Gavade, H. Shinde, A. Gore, P. Mahajan, K. H. Lee, V. Bhuse, K. Garadkar, "An innovative transformation of waste toner powder into magnetic g-C₃N₄-Fe₂O₃ photocatalyst: Sustainable e-waste management," *Journal of Environmental Chemical Engineering*, vol. 7, no. 2, p. 103041, 2019.
- [41] S. Liu, S. Wang, Y. Jiang, Z. Zhao, G. Jiang, Z. Sun, "Synthesis of Fe₂O₃ loaded porous g-C₃N₄ photocatalyst for photocatalytic reduction of dinitrogen to ammonia," *Chemical Engineering Journal*, vol. 373, pp. 572–579, 2019.
- [42] C. Daikopoulos, Y. Georgiou, A. B. Bourlinos, M. Baikousi, M. A. Karakassides, R. Zboril, T. A. Steriotis, Y. Deligiannakis, "Arsenite

- remediation by an amine-rich graphitic carbon nitride synthesized by a novel low-temperature method,” *Chemical Engineering Journal*, vol. 256, pp. 347–355, 2014.
- [43] Y. Yang, J. Chen, Z. Mao, N. An, D. Wang, B. D. Fahlman, “Ultrathin g-C₃N₄ nanosheets with an extended visible-light-responsive range for significant enhancement of photocatalysis,” *RSC Advances*, vol. 7, no. 4, pp. 2333–2341, 2017.
- [44] H. Leelavathi, R. Muralidharan, N. Abirami, S. Tamizharasan, A. Kumarasamy, R. Arulmozhi, “Exploration of ZnO decorated g-C₃N₄ amphiphilic anticancer drugs for antiproliferative activity against human cervical cancer,” *Journal of Drug Delivery Science and Technology*, vol. 68, p. 103126, 2022.
- [45] A. K. Soğuksu, S. Kerli, M. Kavgacı, A. Gündeş, “Electrochemical Properties, Antimicrobial Activity and Photocatalytic Performance of Cerium-Iron Oxide Nanoparticles,” *Russian Journal of Physical Chemistry A*, vol. 96, no. 1, pp. 209–215, 2022.
- [46] F. Shi, L. Chen, C. Xing, D. Jiang, D. Li, M. Chen, “ZnS microsphere/g-C₃N₄ nanocomposite photo-catalyst with greatly enhanced visible light performance for hydrogen evolution: synthesis and synergistic mechanism study,” *RSC Advances*, vol. 4, no. 107, pp. 62223–62229, 2014.
- [47] S. Iqbal, A. Bahadur, S. Ali, Z. Ahmad, M. Javed, R. M. Irfan, N. Ahmad, M. A. Qamar, G. Liu, M. B. Akbar, M. Nawaz, “Critical role of the heterojunction interface of silver decorated ZnO nanocomposite with sulfurized graphitic carbon nitride heterostructure materials for photocatalytic applications,” *Journal of Alloys and Compounds*, vol. 858, p. 158338, 2021.
- [48] S. Le, T. Jiang, Y. Li, Q. Zhao, Y. Li, W. Fang, M. Gong, “Highly efficient visible-light-driven mesoporous graphitic carbon nitride/ZnO nanocomposite photocatalysts,” *Applied Catalysis B: Environmental*, vol. 200, pp. 601–610, 2017.
- [49] S. Sakthivel, B. Neppolian, M. v. Shankar, B. Arabindoo, M. Palanichamy, V. Murugesan, “Solar photocatalytic degradation of azo dye: comparison of photocatalytic efficiency of ZnO and TiO₂,” *Solar Energy Materials and Solar Cells*, vol. 77, no. 1, pp. 65–82, 2003.
- [50] H. Xing, H. Ma, Y. Fu, M. Xue, X. Zhang, X. Dong, X. Zhang, “Preparation of g-C₃N₄/ZnO composites and their enhanced photocatalytic activity,” *Materials Technology*, vol. 30, no. 2, pp. 122–127, 2015.
- [51] Q. Zhong, H. Lan, M. Zhang, H. Zhu, M. Bu, “Preparation of heterostructure g-C₃N₄/ZnO nanorods for high photocatalytic activity on different pollutants (MB, RhB, Cr(VI) and eosin),” *Ceramics International*, vol. 46, no. 8, pp. 12192–12199, 2020.
- [52] X. Li, M. Li, J. Yang, X. Li, T. Hu, J. Wang, Y. Sui, X. Wu, L. Kong, “Synergistic effect of efficient adsorption g-C₃N₄/ZnO composite for photocatalytic property,” *Journal of Physics and Chemistry of Solids*, vol. 75, no. 3, pp. 441–446, 2014.